

RESEARCH PAPER



## p21 limits S phase DNA damage caused by the Wee1 inhibitor MK1775

Sissel Hauge<sup>a</sup>, Libor Macurek<sup>b</sup>, and Randi G. Syljuåsen<sup>b</sup>

<sup>a</sup>Department of Radiation Biology, Institute for Cancer Research, Norwegian Radium Hospital, Oslo University Hospital, Oslo, Norway;

<sup>b</sup>Department of Cancer Cell Biology, Institute of Molecular Genetics of the ASCR, Prague, Czech Republic

### ABSTRACT

The Wee1 inhibitor MK1775 (AZD1775) is currently being tested in clinical trials for cancer treatment. Here, we show that the p53 target and CDK inhibitor p21 protects against MK1775-induced DNA damage during S-phase. Cancer and normal cells deficient for p21 (HCT116 p21<sup>-/-</sup>, RPE p21<sup>-/-</sup>, and U2OS transfected with p21 siRNA) showed higher induction of the DNA damage marker  $\gamma$ H2AX in S-phase in response to MK1775 compared to the respective parental cells. Furthermore, upon MK1775 treatment the levels of phospho-DNA PKcs S2056 and phospho-RPA S4/S8 were higher in the p21 deficient cells, consistent with increased DNA breakage. Cell cycle analysis revealed that these effects were due to an S-phase function of p21, but MK1775-induced S-phase CDK activity was not altered as measured by CDK-dependent phosphorylations. In the p21 deficient cancer cells MK1775-induced cell death was also increased. Moreover, p21 deficiency sensitized to combined treatment of MK1775 and the CHK1-inhibitor AZD6772, and to the combination of MK1775 with ionizing radiation. These results show that p21 protects cancer cells against Wee1 inhibition and suggest that S-phase functions of p21 contribute to mediate such protection. As p21 can be epigenetically downregulated in human cancer, we propose that p21 levels may be considered during future applications of Wee1 inhibitors.

### ARTICLE HISTORY

Received 14 November 2018

Revised 14 February 2019

Accepted 6 March 2019

### KEYWORDS

Wee1 kinase; checkpoint kinase inhibition; p21 (Cip1/Waf1); cancer treatment; DNA damage; CDK activity


## Introduction

Cyclin dependent kinases (CDKs) in complex with different cyclins propel the progression of the cell cycle, and the activity of CDKs is therefore subject to strict regulation. Wee1 kinase phosphorylates CDK1 on tyrosine 15, and thereby restrains CDK activity in G2 phase [1,2]. Accordingly, inhibition of Wee1 causes G2 checkpoint abrogation [3,4]. Based on this, the Wee1 inhibitor MK1775 (AZD1775) is in clinical trials for cancer treatment in combination with radiotherapy or chemotherapeutic drugs [4]. Particularly, G2 checkpoint abrogation by MK1775 may be toxic for p53 mutated cancer cells lacking the p53-dependent G1 checkpoint [3]. However, Wee1 also plays a role in restraining CDK activity in S phase, through tyrosine 15 phosphorylation of both CDK1 and CDK2 [5–7]. Loss of Wee1 during S phase leads to aberrant CDK activity followed by unscheduled replication initiation and subsequent DNA damage [7,8]. Such S phase damage has been termed replication catastrophe [9] and is likely a major cause behind single-agent antitumor activity of Wee1 inhibitors

[10]. The mechanism of how Wee1 inhibition causes this DNA damage in S phase is not completely understood. Furthermore, more knowledge is needed about which factors contribute to resistance or sensitivity towards Wee1 inhibitors.

The p53 target and CDK inhibitor p21 plays a fundamental part in regulating cell cycle progression, as well as cellular senescence and apoptosis [11]. Although p21 mutations are uncommon, emerging evidence has shown that p21 expression can be low in cancer due to epigenetical suppression [12–16]. p21 inhibits CDK activity by binding cyclin-CDK complexes, and thereby induces the G1 checkpoint after DNA damage [17–19]. In addition, p21 has also been implicated in G2 checkpoint maintenance [20]. Furthermore, p21 has a strong affinity for PCNA, and prevents replication by blocking the interaction between PCNA and factors that are necessary for replication, such as replicative DNA polymerases [21,22]. For this reason, p21 levels are reduced in S-phase in order for replication to occur. However, the remaining p21 may have important S-phase functions, as it is

**CONTACT** Randi G. Syljuåsen  [randi.syljuasen@rr-research.no](mailto:randi.syljuasen@rr-research.no)

 Supplemental data for this article can be accessed [here](#)

© 2019 The Author(s). Published by Informa UK Limited, trading as Taylor & Francis Group.

This is an Open Access article distributed under the terms of the Creative Commons Attribution-NonCommercial-NoDerivatives License (<http://creativecommons.org/licenses/by-nc->

involved in regulating translesion synthesis (TLS), limiting unscheduled use of the error-prone TLS polymerases [23]. Recently, p21 has also been implicated in regulation of replication fork progression, although different results were reported as to whether p21 promotes DNA elongation [24] or suppresses fork speed [25].

Interestingly, previous studies have demonstrated that p21 status is important for the responses to a combination of Checkpoint kinase 1 (Chk1) inhibition and irinotecan or gemcitabine [26,27]. Cells deficient for p21 showed more DNA damage and cell death after Chk1 inhibition than p21 proficient cells, but the mechanism behind the increased damage was not known [26,27]. Inhibition of Chk1, similar as for Wee1 inhibition, causes unscheduled replication initiation and DNA damage in S phase [28–30]. Taken together, this led us to investigate whether p21 status also affects the cellular responses to Wee1 inhibition, and whether S phase effects might be involved. Our study shows that loss of p21 leads to more S phase DNA damage and cancer cell death after Wee1 inhibition. These results could be of importance to guide the future clinical implementation of Wee1 inhibitors, as tumors with low p21 expression may be particularly sensitive.

## Materials and methods

### Cell culture, drug treatments and radiation

Human U2OS osteosarcoma cells, HCT116 colon cancer cells and Retinal Pigmented Epithelial (RPE) cells were cultured in DMEM (Dulbecco's modified Eagle's) (U2OS, HCT116) or DMEM/F12 (RPE) medium (both from Invitrogen), supplemented with 10% fetal bovine serum (FBS) and 1% Penicillin/Streptomycin (P/S) at 37°C in a humidified atmosphere with 5% CO<sub>2</sub>. The Wee1 inhibitor MK1775 (AZD1775) (Merck Calbiochem) was used at concentrations from 25nM to 1000nM. The Chk1 inhibitor AZD7762 (Selleck Chemicals) was used at 10nM to 400nM, and Nocodazole (Sigma) was used at 0.04 µg/ml. Irradiation of cells was performed with an X-ray generator (Faxitron CP160, 160 kV, 6.3 mA) at a dose-rate of 1 Gy/min. Cells were irradiated immediately after addition of MK1775.

### p21 siRNA transfection and isogenic cell lines

U2OS cells were transfected with a pool of 4 siRNAs (SMARTpool) targeting p21 (CDKN1a), sequences: GAUGGAACUUCGACUUUGU, GCG AUGGAACUUCGACUUU, CGAUGGAACUUCGACUUUG and CGACUGUGAUGCGCUAACG (Sigma). Alternatively, an independent p21 siRNA was used when indicated (p21siRNA #2); Mission siRNA CDK1NA (p21), sequence: CUAAGAG UGCUGGGCAUUU (Sigma). Cells were subjected to treatment 48 hours post transfection. The HCT116 wild type (wt) and p21 negative (p21<sup>-/-</sup>) cell lines were purchased from Horizon Discovery (HD R02-035), and p21 loss was verified by measuring p21 induction after radiation. RPE cells deficient for p21 were made by the CRISPR/cas9 method: To knock-out the CDKN1A gene, hTERT RPE-1 cells were transfected with a combination (1:1) of p21 CRISPR/Cas9 KO Plasmid (Santa Cruz, sc-400,013), and p21 HDR Plasmid and stable clones were selected by puromycin (10 µg/ml). Integration of the HDR cassette to the CDKN1A locus was confirmed by sequencing, and loss of p21 expression by immunoblotting.

### Flow cytometry

For analysis of protein expression in single cells, cells were fixed with 70% ethanol and stained with antibodies as described previously [31,32]. The antibodies used were mouse anti-phospho-Histone H2AX (Ser139) (γH2AX) (05–636, Millipore), rabbit anti-phospho-RPA (Ser4/Ser8)(A300-245, Bethyl Laboratories), rabbit anti-phospho-Histone H3 (Ser10) (06–570, Millipore), rabbit anti-phospho-BRCA2 (Ser3291) (AB9986, Millipore), rabbit anti-phospho-B-Myb (Thr487) (ab76009, Abcam), mouse anti-phospho-Ser/Thr-Pro MPM-2 (05–368, Millipore) and goat anti-R2 (sc-10,846, Santa Cruz). Secondary antibodies were Alexa Fluor 488 and 647 (Molecular Probes), Dylight 549 (VectorLabs) and Cy3 (Jackson ImmunoResearch) anti-mouse, anti-rabbit and anti-goat IgG. The directly conjugated antibody FITC conjugated anti-phospho-Histone H2AX (Ser139) (Millipore) was used where indicated. When indicated in the figure legend, barcoding was used as before [31–33] to eliminate variation

in antibody staining between individual samples. The DNA stain FxCycle™ Far Red (200nM FxCycle and 0.1 mg/ml RNase A) (Thermo Fisher Scientific) was used for the barcoding, EdU and Pacific Blue-viability experiments, and Hoechst 33258 (1.5µg/ml) (Sigma-Aldrich) for other experiments. For estimations of cell viability, cells were harvested and stained with Pacific Blue (1.5 ng/µl) for 15 minutes at 4°C, before fixation in 70% EtOH (Pacific Blue is a non-permeable stain, so Pacific Blue-positive cells have lost membrane integrity, *i.e.* they are non-viable). For EdU incorporation experiments, the Click-iT™ EdU Alexa Fluor™ 488 Flow Cytometry Assay Kit (Thermo Fisher Scientific) was used according to manufacturers description. Flow cytometry analysis was performed on a LSRII flow cytometer (BD Biosciences) using Diva software, in the Flow Cytometry Core Facility at The Norwegian Radium Hospital. Estimation of cell cycle phase distribution was performed using FlowJo software and the Watson (Pragmatic) univariate model.

#### **Celltiter-glo® and realtime-glo™ assays**

500 U2OS cells (non-transfected or p21siRNA transfected), and 500 or 700 HCT116 cells (wt or p21<sup>-/-</sup> cells, respectively), were seeded in 96 well plates (Sigma Aldrich, CLS3610-48EA) in medium containing inhibitors of indicated concentrations. When indicated, irradiation was performed directly after seeding. The RealTime-Glo kit (Promega) was used for viability assessment in U2OS cells 4–6 days later, and the results presented here are from the 4 days time point (similar results were obtained at the 5 and 6 days time points). The CellTiter-Glo kit (Promega) was used for assessing viability in HCT116 cells at 6 days. Relative viability was calculated in each experiment by mean luminescence signal of treated samples (duplicates were seeded for each condition) divided by mean luminescence signal of non-treated sample (or single-treated sample in the case of drug combination experiments).

#### **Clonogenic survival assays**

U2OS cells were either mock transfected or transfected with p21 siRNA. 48 hours after transfection, the cells were harvested and re-seeded at low density in 6cm

culture dishes (BD Biosciences) with medium containing the Wee1 inhibitor MK1775 (100 or 300 nM). After 24 hours the cells were washed and new medium was added. Cells were then cultured for 14 days, fixed in 70% ethanol and stained with methylene blue. HCT116 cells (wt or p21<sup>-/-</sup>) were seeded at low density in 6cm dishes, and after approximately 20 hours MK1775 (600 or 1000 nM) was added. 24 hours later the cells were washed and new medium was applied. Cells were then cultured for 11 (wt) or 13 (p21<sup>-/-</sup>) days, fixed in 70% ethanol and stained with methylene blue. Colonies of 50 or more cells were counted as survivors. Survival fractions were calculated in each experiment as the average cloning efficiency (from 3 parallel dishes) after treatment with the inhibitors, divided by the average cloning efficiency for non treated cells. Thereafter the survival fraction of p21 deficient cells was calculated relative to the survival fraction of p21 proficient cells.

#### **Immunoblotting**

Cells were lysed in SDS boiling buffer (2% SDS, 10mM Tris-HCl pH 7.5, 100µM Na<sub>3</sub>VO<sub>4</sub>), and immunoblotting was performed as described previously [32]. The following antibodies were used for blotting: rabbit anti-p21 (SC-756, Santa Cruz), mouse anti-CDK1 (9112, Cell Signaling), rabbit anti-Actin (A-5060, Sigma), rabbit anti-phospho-DNA-PKcs (S2056) (ab18192, Abcam), rabbit anti-phospho RPA (S4/S8) (A300-245) (Bethyl Laboratories), mouse anti-gamma-Tubulin (T6557, Sigma) and mouse anti-MCM7 (SC-65,469, Santa Cruz).

#### **Statistical analysis**

Statistical comparisons were made by Two-sample *t* tests. *P* < 0,05 was considered significant. Error bars represent standard error of mean (*N* = 3), unless otherwise stated in the figure legend.

## **Results**

### **p21 deficiency causes increased DNA damage in S phase after wee1 inhibition**

We previously showed that Wee1 inhibition by MK1775 causes DNA breakage in S phase cells

[8,32]. To address whether p21 could protect against such damage, we applied three isogenic cell systems for p21: HCT116 colorectal cancer (wt/p21<sup>-/-</sup>), immortalized normal epithelial RPE (wt/p21<sup>-/-</sup>) and U2OS osteosarcoma with and without p21 siRNA transfection. Lack of p21 expression was verified by Western blotting (Figure 1(a)). The cells were treated with MK1775 for 24 hours, and the DNA damage marker  $\gamma$ H2AX and cell cycle phase was assayed in individual cells by flow cytometry analysis. In all three systems, the p21 depleted cells showed significantly more DNA damage in S phase after MK1775 treatment compared to p21 proficient cells, as seen by a higher amount of S phase cells with strong  $\gamma$ H2AX levels (Figure 1(b)). This was not due to a higher fraction of cells in S phase prior to MK1775 treatment, as the percentages of S phase cells were largely similar for the p21 deficient and proficient cells (Figure S1A). However, consistent with more replication damage, the U2OS cells deficient for p21 accumulated more in S phase upon MK1775 treatment (Figure 1(b), DNA profiles, U2OS 300nM MK1775). Likewise, HCT116 p21<sup>-/-</sup> cells accumulated more in late S/G2 phase after MK1775 treatment, also in agreement with more replication damage (Figure 1(b), DNA profiles, HCT116 600nM and 1000nM MK1775). We have previously observed that different cell lines accumulate at various stages of S-phase upon Wee1 inhibition (unpublished observations). Although the HCT116 cells accumulate at a later stage than U2OS cells after treatment, we believe the problems still arise during replication, as the median values of  $\gamma$ H2AX signals increase in EdU positive (S phase) HCT116 cells after increasing doses of MK1775 (Figure S1B). In these experiments we applied lower concentrations of MK1775 for U2OS cells (100–300nM) compared to the two other cell lines (600–1000nM), because U2OS cells are highly sensitive to MK1775-induced S phase DNA damage [32]. Next, we measured phosphorylation of DNA-PKcs S2056 and RPA S4/S8 by Western Blotting, common markers for DNA double strand breaks (DSBs) and replication stalling, respectively [34,35]. Consistent with the results for  $\gamma$ H2AX, the p21 negative cells showed stronger phosphorylation of both DNA-PKcs S2056 and RPA S4/S8 after MK1775 treatment compared to the p21 proficient cells (Figure 1(c)). The enhanced phosphorylation of RPA S4/S8 in p21 deficient U2OS cells was verified by

flow cytometry analysis (Figure S2). Furthermore, simultaneous analysis of both phospho-RPA S4/S8 and  $\gamma$ H2AX revealed that the S phase cells with strong phospho-RPA S4/S8 also displayed strong  $\gamma$ H2AX levels, and vice versa (Figure S2). Taken together, these results show that p21 protects cells from DNA damage in S phase after Wee1 inhibition.

### ***The increased DNA damage in p21 deficient cells occurs specifically in S phase, but is not caused by elevated CDK activity***

Because of the important role of p21 in controlling the transition from G1 to S phase, we asked whether the cells with high DNA damage might potentially have aberrantly entered from G1 into S phase during MK1775 treatment. To address this issue, we first treated p21 positive and negative U2OS and RPE cells with MK1775 in the presence of Nocodazole, a microtubule inhibitor which stops cells in mitosis and thereby prevents the cells from proceeding into a second G1 and S phase during the 24 hours treatment of Wee1 inhibition. Notably, the number of cells with strong  $\gamma$ H2AX levels in S-phase was higher for the p21 negative cells also in the presence of Nocodazole (Figure 2(a)). Hence, the increased DNA damage in p21 deficient cells arises in the first S phase during MK1775 treatment. Furthermore, we performed a different set of experiments where U2OS ( $\pm$  p21 siRNA) and HCT116 (wt/p21<sup>-/-</sup>) cells were treated with a pulse of the thymidine analogue 5-Ethynyl-2'-deoxyuridine (EdU) immediately before adding the Wee1 inhibitor, and the  $\gamma$ H2AX levels and cell cycle profiles of EdU positive cells were assayed at 6 or 10 hours later, respectively. In this way we could follow the fate of cells that were in S phase at the time of adding MK1775, thus excluding all cells that were entering S phase from G1 phase during the treatment. Again, more p21 deficient cells showed strong  $\gamma$ H2AX levels than p21 proficient cells (Figure 2(b), top). In addition, the resulting cell cycle profiles of the EdU positive populations showed that p21 deficient S phase cells had more trouble progressing through the cell cycle after MK1775 treatment than p21 proficient S phase cells (Figure 2(b), bottom). These results demonstrate that the increased DNA damage in p21 negative cells is not caused by cells entering aberrantly from G1 into S phase during

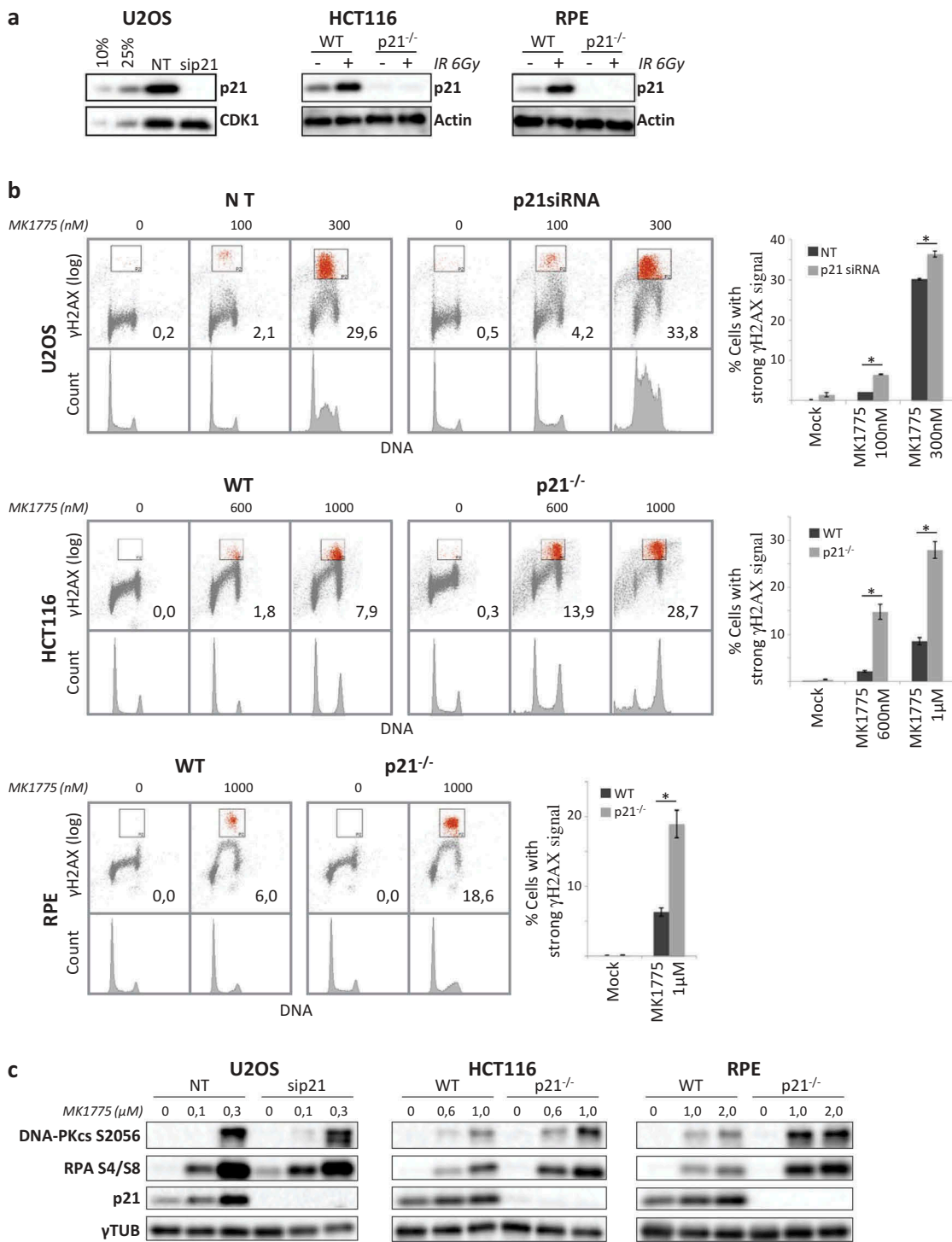


**Figure 1.** p21 deficiency causes increased DNA damage in S phase after Wee1 inhibition.

(a). Immunoblot analysis showing p21 knockdown efficiency in U2OS cells, and confirming p21 knockout in HCT116 and RPE cells. U2OS cells were harvested 48 hours after transfection with p21 siRNA. The two first lanes in the U2OS blot were loaded with 10% and 25% of the mock transfected sample (NT). HCT116 wt/p21<sup>-/-</sup> and RPE wt/p21<sup>-/-</sup> cells were irradiated with 6 Gy and harvested after 4 hours. CDK1 or Actin were used as loading controls. (b). Flow cytometric analysis of U2OS (mock (NT) or p21 siRNA transfected), HCT116 wt/p21<sup>-/-</sup> and RPE wt/p21<sup>-/-</sup> cells treated for 24 hours with MK1775. Scatter plots of  $\gamma$ H2AX versus Hoechst (DNA) and the corresponding DNA histograms are shown from representative experiments. Numbers are the percentage of cells within the indicated region with strong  $\gamma$ H2AX signal (red color). The graphs to the right show the mean percentage of cells with strong  $\gamma$ H2AX signals. Error bars: SEM (N  $\geq$  3). \*P < 0,05. (c). Immunoblot analysis showing double strand break signaling in U2OS (mock (NT) or p21 siRNA transfected), HCT116 wt/p21<sup>-/-</sup> and RPE wt/p21<sup>-/-</sup> cells after 24 hours of MK1775 treatment at the indicated concentrations.

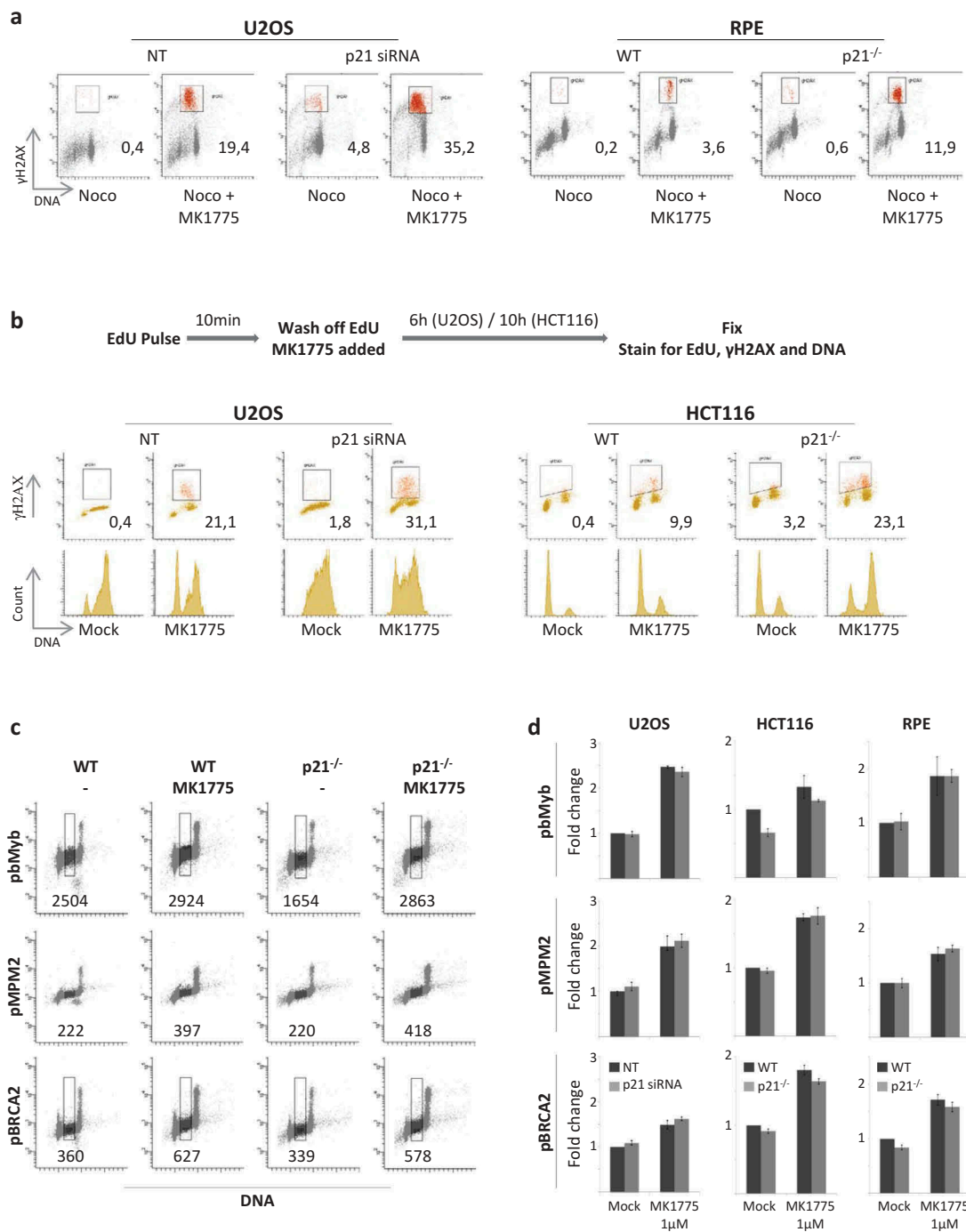


**Figure 2.** The increased DNA damage in p21 deficient cells occurs specifically in S phase, but is not caused by elevated CDK activity. (a). Flow cytometric analysis of U2OS (mock (NT) or p21 siRNA transfected) and RPE (wt/p21<sup>-/-</sup>) cells treated with MK1775 (20 hours with 300nM and 24 hours with 1μM, respectively) and Nocodazole simultaneously. Scatter plots of γH2AX versus Hoechst (DNA) are shown from representative experiments. Numbers are the percentage of cells within the indicated region with strong γH2AX signal (red color). (b). Flow cytometric analysis of U2OS (mock (NT) or p21 siRNA transfected) and HCT116 wt/p21<sup>-/-</sup> cells treated as shown in the work flow at the top. The S-phase population was first labeled with a short EdU pulse, and then cells were washed and treated with 1μM MK1775 (MK1775) or left untreated (Mock). At 6 or 10 hours later (for U2OS and HCT116 cells, respectively), samples were fixed and stained for γH2AX, EdU and DNA content. Scatter plots showing γH2AX versus FxCycle (DNA) for EdU positive cells, are presented in the top row. Numbers are the percentage of cells within the indicated region with strong γH2AX signal (red color). Associated DNA histograms of EdU positive cells are shown in the bottom row. Note that the scatter plots and DNA histograms include only the EdU positive cells (which were in S phase 6 or 10 hours earlier). (c and d). Flow cytometric analysis of CDK-dependent phosphorylations in S phase cells. U2OS cells mock transfected (NT) or transfected with p21 siRNA, HCT116 wt/p21<sup>-/-</sup> and RPE wt/p21<sup>-/-</sup> cells were treated with 1μM MK1775 for 90 minutes, or left untreated (Mock). Samples were bar-coded with Pacific Blue before antibody staining with the indicated antibodies. Scatter plots of phospho-B-Myb (T487), phospho-Ser/Thr-Pro MPM-2 and phospho-BRCA2 (S3291) versus FxCycle (DNA) shown in C., are from a representative experiment in the HCT116 isogenic cell system. S-phase cells are indicated in dark color, and numbers are median signal values in the S phase gates, with background signals subtracted. Graphs in D. show average median values in S-phase (relative to Mock) for all cell lines. Error bars: SEM (N = 3 (2 in HCT116 cells)).

MK1775 treatment. Rather, the increased DNA damage occurs as a consequence of events occurring in S phase upon MK1775 treatment.

As unscheduled CDK activity is thought to mediate MK1775-induced DNA damage in S phase, and both p21 and Wee1 are well known CDK inhibitors [2,5,11], we next addressed whether the increased DNA damage observed in p21 negative cells might be caused by increased CDK activity. We previously developed a flow cytometry based assay to measure CDK activity during specific cell cycle phases, by examining CDK-dependent phosphorylations [31,32]. Using this method, we measured S phase CDK activity after 90 minutes of MK1775 treatment in p21 positive and negative U2OS, HCT116 and RPE cells. As expected and in concordance with previous studies [32], Wee1 inhibition caused increased phosphorylation of all three markers in the assay (Figure 2(c,d)). However, this CDK activity was not further increased in p21 negative cell lines (Figure 2(c,d)), suggesting that loss of p21 does not cause increased CDK activity during S phase. Moreover, it has been shown that increased CDK activity upon Wee1 inhibition causes decreased levels of the Ribonucleotide Reductase subunit R2, which is essential for nucleotide production [36]. Consistent with the CDK activity results above, we observed a similar decrease in R2 levels after MK1775 treatment in p21 positive and negative cells (Figure S3A and B). Of note, transient depletion of p21 by siRNA in U2OS cells did cause a decrease in R2 levels (data not shown), but the MK1775-induced decrease was not bigger than in p21 proficient cells. Altogether, these results suggest that an S phase function of p21 can protect against MK1775-induced DNA damage, but this protection is not due to an effect of p21 in restraining S phase CDK activity.

### **Effects of p21 status on mitotic entry and G1-arrest after Wee1 inhibition**

We next asked whether p21 status might also be important for mitotic entry or G1-arrest after MK1775 treatment. We performed flow cytometric analysis of the percentage of mitotic cells at 90 minutes and 24 hours after Wee1 inhibition in p21

positive and negative cells. As expected, the number of mitotic cells was increased after MK1775 treatment in all three cell systems (Figure 3(a,b)), consistent with MK1775-induced mitotic entry. However, the effects of p21 loss on mitotic entry after MK1775 treatment varied between the cell lines and with different concentrations of the Wee1 inhibitor (no effects in U2OS cells; some effects in HCT116 and RPE cells) (Figure 3(a,b)). Furthermore, the majority of the cells with strong S phase  $\gamma$ H2AX were not positive for the mitotic marker phospho-H3 Ser10 and most of the mitotic cells were negative for  $\gamma$ H2AX (Figure 3(c)), indicating that the S phase DNA damage and mitotic entry are two separate effects after MK1775 treatment. Moreover, few cells showed induction of premature mitosis (H3P positive cells with  $<4N$  DNA content) after Wee1 inhibition, and p21 loss did not seem to increase this amount further (Figure 3(c) lower panels). The latter is in agreement with the CDK activity measurements above, where we observed no increase in S phase CDK activity in p21 negative cells compared to p21 positive cells after Wee1 inhibition (Figure 2(c,d) and S3). Next, we wanted to address whether Wee1 inhibition could induce a p21 dependent first or second-cycle G1-arrest. To examine first cycle G1-arrest, we compared the G1 population after 24 hours treatment with MK1775 and Nocodazole to the G1 population after treatment with Nocodazole alone. The results showed no indication of a strong first cycle G1-arrest in any of the cell lines (Figure 3(d)). To measure second-cycle G1-arrest, we first treated the cells with MK1775 for 24 hours, followed by Nocodazole for the next 24 hours (Figure 3(e)). Again, there was no indication of a strong G1-arrest after Wee1 inhibition in p21 positive or negative cancer cells, but the p21 positive RPE cells showed some G1 accumulation in the second cycle which was abrogated by loss of p21 (Figure 3(e), bottom panels: 26.5% versus 8.8% G1 cells for RPE wt and p21<sup>-/-</sup> cells, respectively). Taken together, these results show that the effects of Wee1 inhibition on mitotic entry and G1-arrest vary between cell lines, but overall, the differences in these responses between p21 proficient and deficient cells are less pronounced than the differences in S phase DNA damage (Figure 1). We conclude that a major consequence of p21 deficiency is

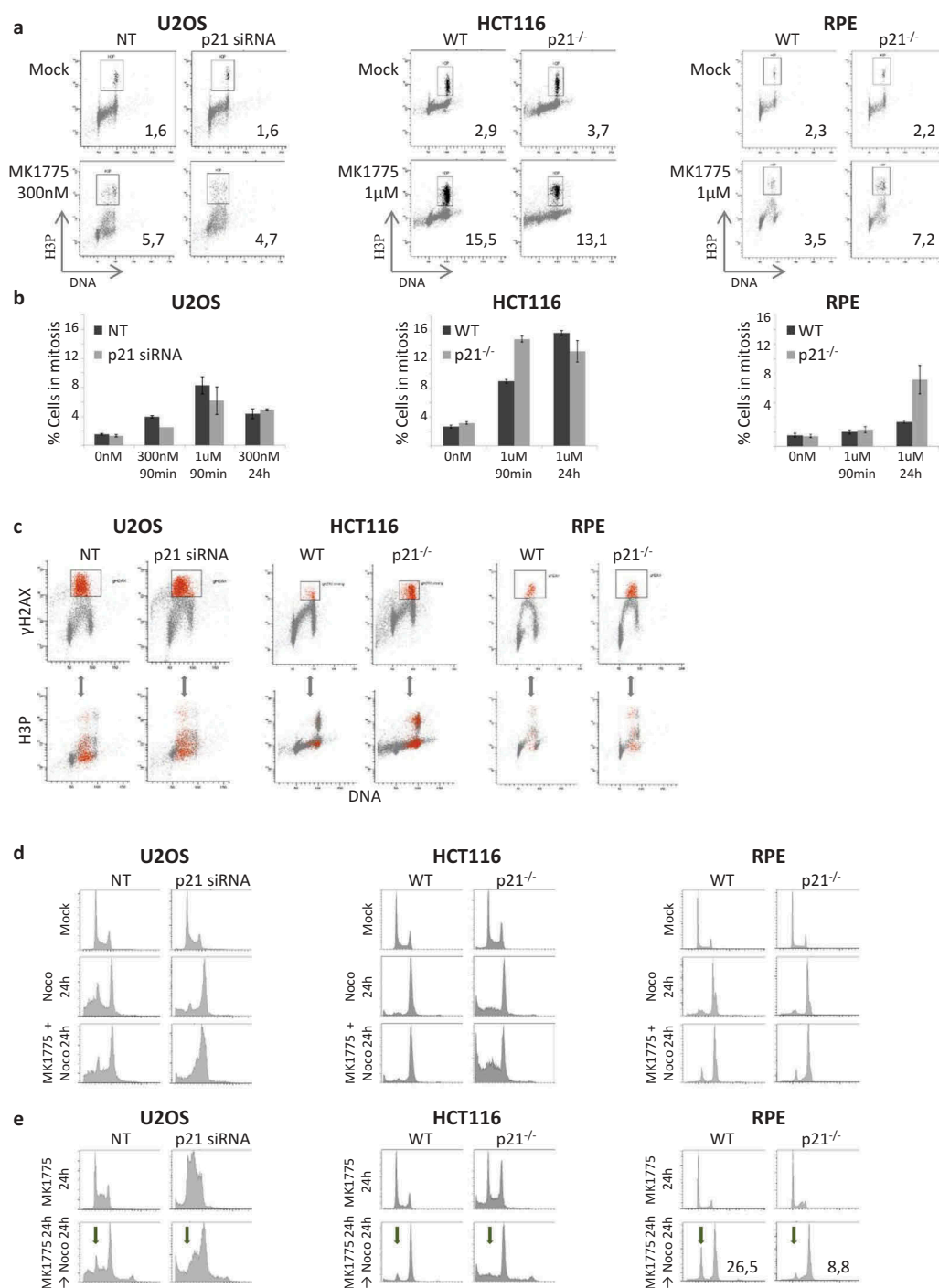


**Figure 3.** Effects of p21 status on mitotic entry and G1/S arrest after Wee1 inhibition.

(a). Flow cytometric analysis of U2OS (mock (NT) or p21 siRNA transfected), HCT116 wt/p21<sup>-/-</sup> and RPE wt/p21<sup>-/-</sup> cells treated for 24 hours with MK1775 at the indicated concentrations. Scatter plots of phospho-Histone H3 (S10) versus Hoechst (DNA) are shown from representative experiments. Numbers are the percentage of cells within the indicated region of mitosis (in black). (b). The mean percentage of mitotic cells after indicated MK1775 concentrations and time-points, from experiments analyzed as in A. Of note, for the 90 minutes time-points, mitotic cells were measured by phospho-B-Myb (T487). Error bars: Standard error of mean (SEM) (N = 2–3). (c). Scatter plots of γH2AX versus Hoechst (DNA), and phospho-Histone H3 (S10) versus Hoechst (DNA) from the same experiments as in A. The cells with strong γH2AX signal (red color) are also shown in red in the phospho-Histone H3 plots. (d). U2OS (mock (NT) or p21 siRNA transfected), HCT116 wt/p21<sup>-/-</sup> and RPE wt/p21<sup>-/-</sup> cells were mock treated or treated for 24 hours with Nocodazole alone or Nocodazole and MK1775 (300nM in U2OS, 600nM in HCT116 and 1μM in RPE cell systems). Samples were analyzed by flow cytometry, and the histograms show the DNA profiles of representative experiments. (e). Cells were treated for 24 hours with MK1775 (300nM, 600nM and 1μM, respectively) and fixed (top row) or washed and subsequently grown for 24 additional hours in the presence of Nocodazole (bottom row). Arrows in the bottom panels indicate where cells arrested at a second cycle G1 checkpoint would be present.



increased S phase DNA damage in response to the Wee1 inhibitor MK1775.

### **p21 protects cancer cells against Wee1 inhibition induced cell death**

As mentioned above, p21 expression can be low in human tumors due to epigenetical suppression [12–16]. To address whether p21 might protect cancer cells from MK1775-induced cell death, we examined cell growth and viability and clonogenic survival of the p21 positive and negative U2OS and HCT116 cells. We first measured loss of cell viability by assessing the uptake of the non-permeable dye Pacific Blue at 3 days after treatment with MK1775 for 24 hours. Higher numbers of non-viable cells were observed after MK1775 treatment in p21 deficient compared to p21 proficient U2OS and HCT116 cells (Figure 4(a, b)). Similar effects were observed by measuring the percentage of cells with sub-G1 DNA content (Figure 4(c,d)). These effects were supported by CellTiterGlo/RealTimeGlo growth assays, which showed reduced growth in the p21 deficient U2OS and HCT116 cells after MK1775 treatment compared to p21 proficient cells (Figure 4(e)). Note that in the latter experiments the inhibitor was not washed off, but present for several days, and we therefore used lower concentrations of MK1775. Of note, the lowest concentrations (25–50 nM) slightly increased growth in p21 positive U2OS cells (Figure 4(e)). Such growth stimulation has also been reported previously and is likely a cell type dependent effect associated with shortening of the cell cycle after treatment with low and non-lethal concentrations of the Wee1 inhibitor [37]. Finally, we performed clonogenic survival assays in HCT116 and U2OS cells and observed reduced survival of p21 negative compared to p21 positive cells upon Wee1 inhibition (Figure 4(f,g)). We conclude that for U2OS and HCT116 cancer cells, p21 deficiency leads to increased cell death in response to MK1775 treatment.

Similar to Wee1 inhibition, inhibition of Chk1 also causes DNA damage in S phase [29], and we recently showed that simultaneous inhibition of both Chk1 and Wee1 synergistically increases such damage [32]. As we found that p21 deficiency enhanced the S phase DNA damage and cell death after Wee1 inhibition (Figures 1, 2 and 4), we reasoned that similar effects might be observed in response to

Chk1 inhibition and upon simultaneous Chk1/Wee1 inhibition. To address this issue, we assayed cell growth by the CellTiterGlo/RealTimeGlo assays and  $\gamma$ H2AX levels by flow cytometry. Cell growth after treatment with the Chk1 inhibitor AZD7762 was slightly more reduced in p21 deficient U2OS and HCT116 cells compared to p21 proficient cells (Figure 5(a)). Furthermore, the p21 deficient U2OS and HCT116 cells were more sensitive to the combined treatment of MK1775 and AZD7762 (Figure 5(b)). The number of cells with strong  $\gamma$ H2AX levels was also higher in p21 deficient HCT116 and U2OS cells after the combined treatment (Figure 5(c)), consistent with increased S phase DNA damage. These results show that p21 also protects against the S phase DNA damage in response to Chk1 inhibition or combined Chk1/Wee1 inhibition.

Finally, as Wee1 inhibitors are typically applied together with DNA damaging agents such as ionizing radiation, we also assessed the growth of p21 deficient and proficient U2OS and HCT116 cells upon treatment with 2 Gy of X-ray irradiation in combination with various concentrations of MK1775. Again, cell growth was most reduced in the p21 negative cancer cells (Figure 5(d)), indicating that p21 deficiency can also sensitize cancer cells to combination treatments of MK1775 with radiation.

## **Discussion**

In this study we report that the p53 target and CDK inhibitor p21 can protect cells from S phase DNA damage induced by the Wee1 inhibitor MK1775. We also show that p21 deficiency can sensitize cancer cells to MK1775-induced cell death, as measured by cell viability, clonogenic survival and cell growth assays. Moreover, the p21 deficient cancer cells are also more sensitive to combination treatments of MK1775 and the Chk1 inhibitor AZD6772 or MK1775 together with ionizing radiation. Altogether these results provide a rationale for the application of Wee1 inhibitors in tumors with low levels of p21, and support recent studies indicating that p21 can have important functions in S phase.

p21 is known as a CDK inhibitor important in the G1 and G2 phases of the cell cycle. As p21 levels are low in S phase, the investigation into the

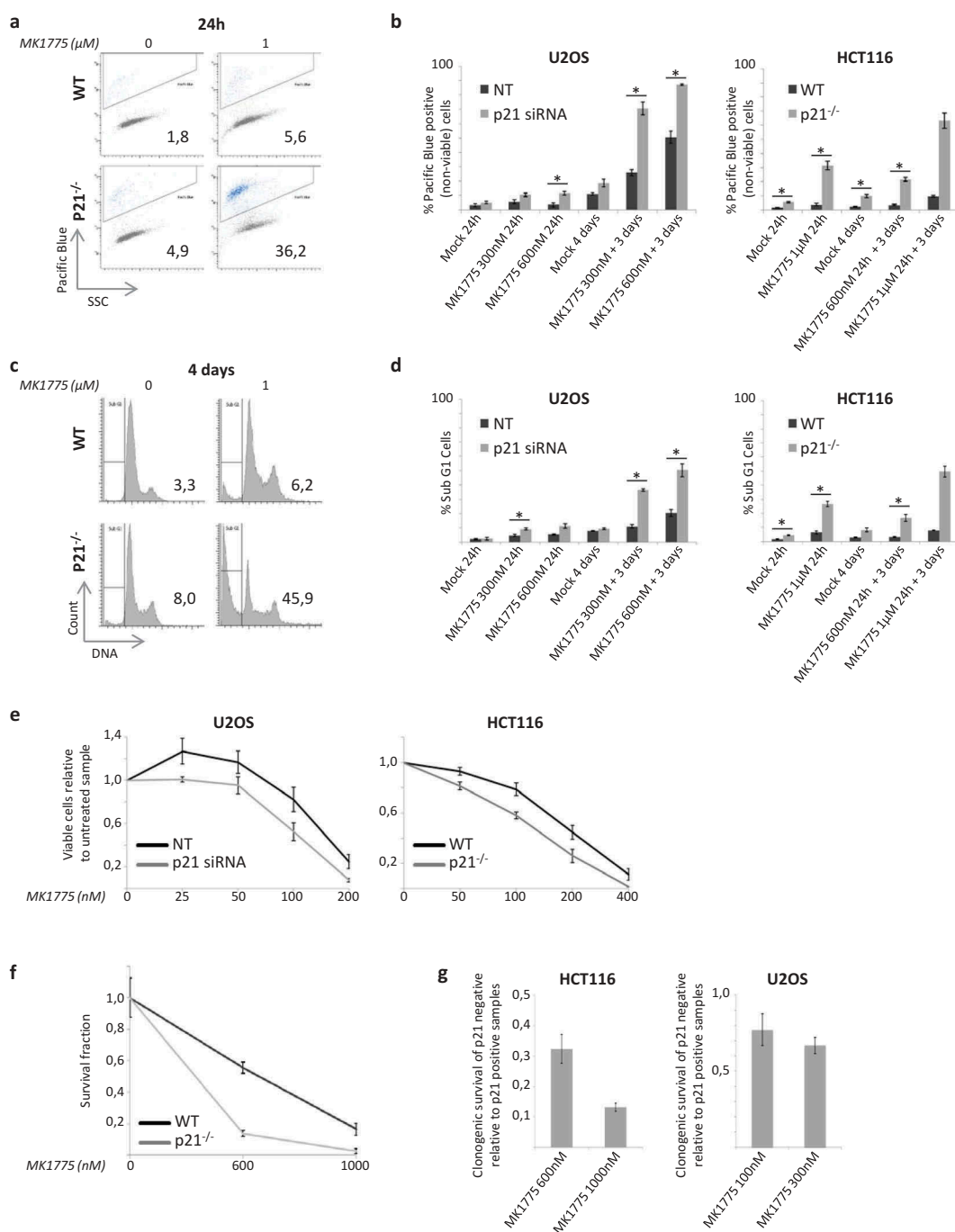


**Figure 4.** p21 protects cancer cells against Wee1 inhibition induced cell death.

(a and b). U2OS cells mock transfected (NT) or transfected with p21 siRNA, and HCT116 wt/p21<sup>-/-</sup> cells were treated with the indicated concentrations of MK1775 for 24 hours. The cells were then either fixed, or washed and then left in fresh medium for three additional days before fixation. Pacific Blue (PB) staining was performed before fixation in order to distinguish viable (PB negative) from non-viable (PB-positive) cells. After staining for DNA content, analysis was performed by flow cytometry. The scatter plots of Pacific Blue versus side scatter presented in A. show a representative experiment from the HCT116 cell line. Numbers indicate the percentage of PB positive cells. The graphs in B. show the mean percentage of PB positive cells after the indicated treatments. Error bars: SEM (N = 3 (2 in HCT116 cells "1 $\mu\text{M}$  24h + 3 days")). \*P < 0,05. (c and d). Calculations of the sub-G1 population in the same experiments as in A and B. DNA histograms in C. show a representative experiment from the HCT116 cell line. Numbers indicate the percentage of cells in the sub-G1 gate. The graphs in D. show the mean percentage of sub-G1 cells after the indicated treatments. Error bars: SEM. (e). Viability of U2OS (mock or p21 siRNA transfected), and HCT116 wt/p21<sup>-/-</sup> cells, measured by the RealTimeGlo (U2OS) or CellTiterGlo (HCT116) assays at 4 and 6 days, respectively, after addition of MK1775 at the indicated concentrations. Error bars: SEM (N = 3). (f). Clonogenic survival assay of HCT116 wt and p21<sup>-/-</sup> cells treated with MK1775 at the indicated concentrations for 24 hours. Results shown are from one representative experiment. Error bars: standard deviation of three parallel dishes. (g). Average survival fractions of p21 deficient relative to p21 proficient cells from three independent experiments in U2OS and HCT116 cells performed as in F. The ratios of survival fractions for p21 siRNA transfected U2OS cells relative to mock, and for HCT116 p21<sup>-/-</sup> cells relative to wt cells, are shown. Error bars: SEM (N = 3 except for HCT116 cells with 1 $\mu\text{M}$  MK1775 (N = 2)).

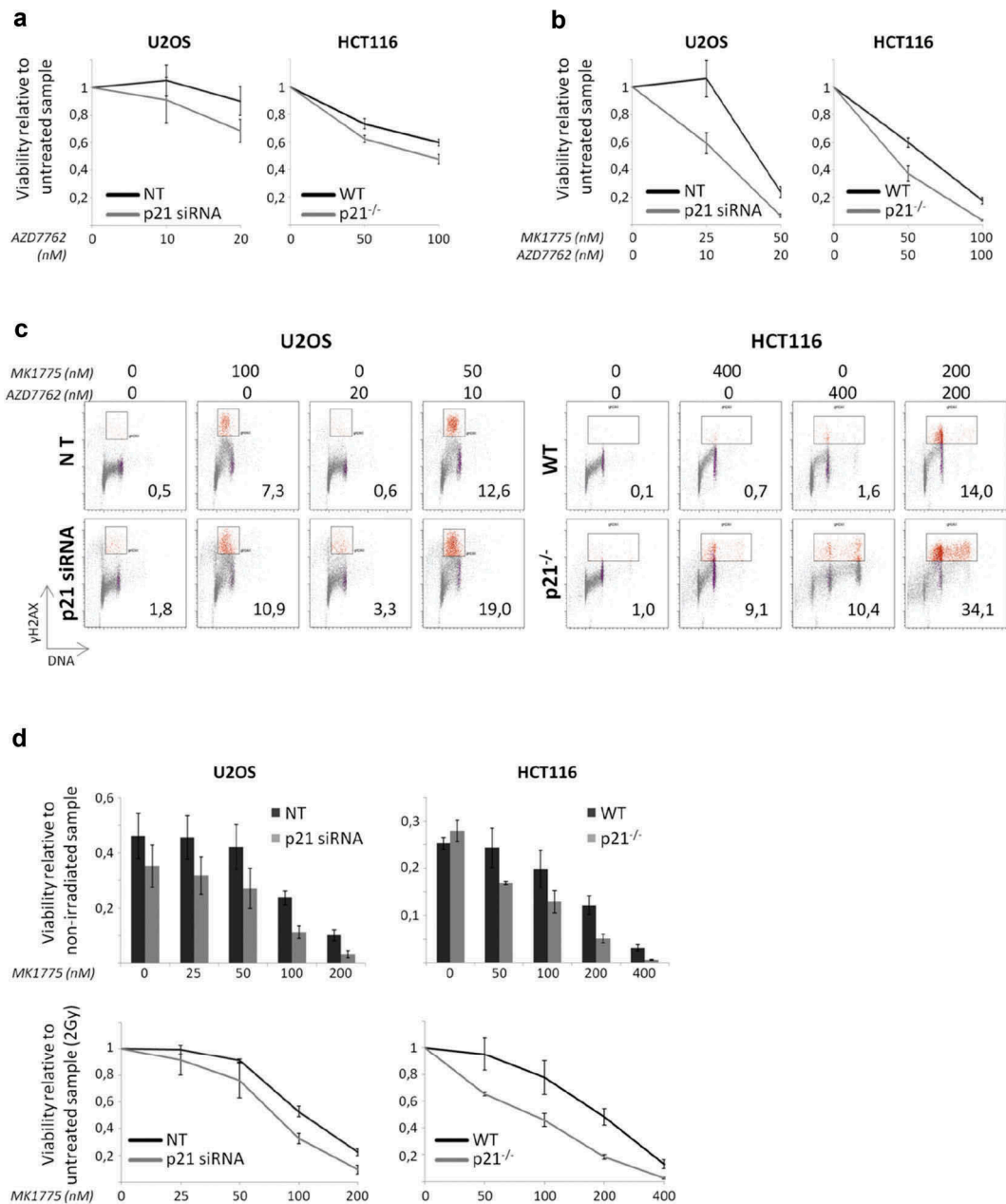


**Figure 5.** Lack of p21 sensitizes cancer cells to combined treatment with Wee1 and Chk1 inhibitors and to the combination of Wee1 inhibition and ionizing radiation.

(a). Viability of U2OS (mock or p21 siRNA transfected), and HCT116 wt/p21<sup>-/-</sup> cells, measured by the RealTimeGlo (U2OS) or CellTiterGlo (HCT116) assays at 4 and 6 days, respectively, after addition of AZD7762 at the indicated concentrations. Error bars: SEM (N = 3 (2 in HCT116 cells 100nM AZD7762)). (b). Viability measured as in A. after addition of MK1775 and AZD7762 at the indicated concentrations. Error bars: SEM (N = 3 (2 in HCT116 cells 100nM AZD7762)). (c). Flow cytometric analysis of U2OS (mock (NT) or p21 siRNA transfected) and HCT116 wt/p21<sup>-/-</sup> cells treated for 24 hours with the Wee1 inhibitor MK1775, the CHK1 inhibitor AZD7762, or the combination of both, in indicated concentrations. Scatter plots of γH2AX versus Hoechst (DNA) are shown from representative experiments. Numbers are the percentage of cells within the indicated region with strong γH2AX signal (red color). (d). Top histograms: Viability of U2OS (mock or p21 siRNA transfected), and HCT116 wt/p21<sup>-/-</sup> cells, measured by the RealTimeGlo (U2OS) or CellTiterGlo (HCT116) assays at 4 and 6 days, respectively, after treatment with MK1775 in the indicated concentrations and X-ray irradiation (2 Gy). Viability was calculated relative to the corresponding non-irradiated p21 proficient or defective sample (such as in Figure 4E). Bottom graphs: Viability was calculated relative to the 2Gy but otherwise untreated samples, for p21 positive and negative cells respectively. Error bars: SEM (N = 3).

role of the remaining p21 in this cell cycle phase has been limited. Considering the acknowledged role of p21 in regulating CDK activity, we wondered whether this role could be important also during S phase when Wee1 is inhibited. Potentially, higher CDK activity after Wee1 inhibition in p21 negative S phase cells could be the cause of the higher DNA damage. However, we did not detect increased CDK activity after p21 loss by our flow cytometric measurements of CDK target phosphorylations (Figure 2(c,d)). Furthermore, S phase levels of the CDK target R2 were also not altered in p21 deficient cells upon Wee1 inhibition (Figure S3). It is therefore likely that other roles of p21 in S phase protects cells from DNA damage after Wee1 inhibition.

Interestingly, we have seen higher EdU uptake in p21 negative compared to p21 positive HCT116 cells, both before and after Wee1 inhibition (Figure S4). This could possibly indicate that p21 is involved in restraining replication when Wee1 mediated restriction of replication is inhibited. Moreover, p21 has been implicated in promoting the Fanconi anemia (FA) DNA repair pathway [38] and regulation of translesion synthesis (TLS) [23]. The latter function could be of special importance, as the TLS factor DNA polymerase kappa has been shown to confer tolerance to Wee1 inhibition [39]. However, we have not been able to see any marked differences in FANCD2 and PCNA ubiquitination between p21 proficient and negative samples after Wee1 inhibition (data not shown). Conceptually, we therefore envision that p21 is involved in restraining replication after Wee1 inhibition, limiting S phase DNA damage and subsequent cell death, but the exact mechanism for how p21 is involved in this remains to be elucidated.

The Wee1 inhibitor MK1775 (now entitled AZD1775) is currently being investigated in more than fifty clinical trials for cancer treatment, as monotherapy or in combination with chemotherapeutic drugs and/or radiation ([www.clinicaltrials.gov](http://www.clinicaltrials.gov)). There is therefore a need for more knowledge about what factors might be of importance with regards to sensitivity to Wee1 inhibition. Several preclinical studies suggest that p53 status may be important for the effects, and recently published results of phase I and II clinical studies

show some enhanced sensitivity in p53 mutated cancers [3,40–44]. There is emerging evidence that the expression of p21, a major p53 target [11], can also be deregulated in cancers, as a result of epigenetic changes [12–16]. This, combined with our finding that p21 protects cancer cells against MK1775 induced death, suggest that p21 expression could be another factor to be taken into consideration when implementing Wee1 inhibition in the treatment of cancer.

## Disclosure statement


No potential conflict of interest was reported by the authors.

## Funding

This research was supported by grants from The Norwegian Cancer Society (62320, 198018), South-Eastern Norway Regional Health Authority (2016114) and the EEA Czech-Norwegian Research Programme -Norwegian Financial Mechanism 2009-2014 (PHOSCAN, 7F14061). LM was supported by the Grant Agency of the Czech Republic (17-04742S).

## ORCID

Libor Macurek  <http://orcid.org/0000-0002-0987-1238>

Randi G. Syljuåsen  <http://orcid.org/0000-0003-3404-6069>

## References

- [1] McGowan CH, Russell P. Cell cycle regulation of human WEE1. *Embo J.* 1995 May 15;14(10):2166–2175. PubMed PMID: 7774574; PubMed Central PMCID: PMCPMC398322.
- [2] Parker LL, Piwnicka-Worms H. Inactivation of the p34cdc2-cyclin B complex by the human WEE1 tyrosine kinase. *Science.* 1992 Sep 25;257(5078):1955–1957. PubMed PMID: 1384126.
- [3] Hirai H, Iwasawa Y, Okada M, et al. Small-molecule inhibition of Wee1 kinase by MK-1775 selectively sensitizes p53-deficient tumor cells to DNA-damaging agents. *Mol Cancer Ther.* 2009 Nov;8(11):2992–3000. PubMed PMID: 19887545.
- [4] Mueller S, Haas-Kogan DA. WEE1 Kinase as a target for cancer therapy. *J Clin Oncol.* 2015 Oct 20;33(30):3485–3487. PubMed PMID: 26215953. .
- [5] Watanabe N, Broome M, Hunter T. Regulation of the human WEE1Hu CDK tyrosine 15-kinase during the cell cycle. *Embo J.* 1995 May 1;14(9):1878–1891. PubMed PMID: 7743995; PubMed Central PMCID: PMCPMC398287.

- [6] Anda S, Rothe C, Boye E, et al. Consequences of abnormal CDK activity in S phase. *Cell Cycle*. 2016;15(7):963–973. PubMed PMID: 26918805; PubMed Central PMCID: PMC4889304. .
- [7] Beck H, Nähse V, Larsen MS, et al. Regulators of cyclin-dependent kinases are crucial for maintaining genome integrity in S phase. *J Cell Biol*. 2010 Mar 8;188(5):629–638. PubMed PMID: 20194642; PubMed Central PMCID: PMC2835936.
- [8] Beck H, Nähse-Kumpf V, Larsen MS, et al. Cyclin-dependent kinase suppression by WEE1 kinase protects the genome through control of replication initiation and nucleotide consumption. *Mol Cell Biol*. 2012 Oct;32(20):4226–4236. PubMed PMID: 22907750; PubMed Central PMCID: PMC3457333.
- [9] Toledo LI, Altmeyer M, Rask MB, et al. ATR prohibits replication catastrophe by preventing global exhaustion of RPA. *Cell*. 2013 Nov 21;155(5):1088–1103. PubMed PMID: 24267891.
- [10] Guertin AD, Li J, Liu Y, et al. Preclinical evaluation of the WEE1 inhibitor MK-1775 as single-agent anticancer therapy. *Mol Cancer Ther*. 2013 Aug;12(8):1442–1452. PubMed PMID: 23699655.
- [11] Karimian A, Ahmadi Y, Yousefi B. Multiple functions of p21 in cell cycle, apoptosis and transcriptional regulation after DNA damage. *DNA Repair (Amst)*. 2016 Jun;42:63–71. PubMed PMID: 27156098.
- [12] Ivanovska I, Ball AS, Diaz RL, et al. MicroRNAs in the miR-106b family regulate p21/CDKN1A and promote cell cycle progression. *Mol Cell Biol*. 2008 Apr;28(7):2167–2174. PubMed PMID: 18212054; PubMed Central PMCID: PMC2268421.
- [13] He Y, Yu B. MicroRNA-93 promotes cell proliferation by directly targeting P21 in osteosarcoma cells. *Exp Ther Med*. 2017 May;13(5):2003–2011. PubMed PMID: 28565800; PubMed Central PMCID: PMC5443279. .
- [14] Bi YY, Shen G, Quan Y, et al. Long noncoding RNA FAM83H-AS1 exerts an oncogenic role in glioma through epigenetically silencing CDKN1A (p21). *J Cell Physiol*. 2018 Jun 5. PubMed PMID: 29870057. DOI:10.1002/jcp.26813.
- [15] Ni N, Song H, Wang X, et al. Up-regulation of long noncoding RNA FALEC predicts poor prognosis and promotes melanoma cell proliferation through epigenetically silencing p21. *Biomed Pharmacother*. 2017 Dec;96:1371–1379. PubMed PMID: 29196104.
- [16] Chen Z, Chen X, Chen P, et al. Long non-coding RNA SNHG20 promotes non-small cell lung cancer cell proliferation and migration by epigenetically silencing of P21 expression. *Cell Death Dis*. 2017 Oct 5;8(10):e3092. PubMed PMID: 28981099; PubMed Central PMCID: PMC5682652.
- [17] Brugarolas J, Chandrasekaran C, Gordon JI, et al. Radiation-induced cell cycle arrest compromised by p21 deficiency. *Nature*. 1995 Oct 12;377(6549):552–557. PubMed PMID: 7566157.
- [18] Chen J, Saha P, Kornbluth S, et al. Cyclin-binding motifs are essential for the function of p21CIP1. *Mol Cell Biol*. 1996 Sep;16(9):4673–4682. PubMed PMID: 8756624; PubMed Central PMCID: PMC231467.
- [19] Deng C, Zhang P, Harper JW, et al. Mice lacking p21CIP1/WAF1 undergo normal development, but are defective in G1 checkpoint control. *Cell*. 1995 Aug 25;82(4):675–684. PubMed PMID: 7664346.
- [20] Bunz F, Dutriaux A, Lengauer C, et al. Requirement for p53 and p21 to sustain G2 arrest after DNA damage. *Science*. 1998 Nov 20;282(5393):1497–1501. PubMed PMID: 9822382.
- [21] Waga S, Hannon GJ, Beach D, et al. The p21 inhibitor of cyclin-dependent kinases controls DNA replication by interaction with PCNA. *Nature*. 1994 Jun 16;369(6481):574–578. PubMed PMID: 7911228.
- [22] Moldovan GL, Pfander B, Jentsch S. PCNA, the maestro of the replication fork. *Cell*. 2007 May 18;129(4):665–679. PubMed PMID: 17512402. .
- [23] Soria G, Speroni J, Podhajcer OL, et al. p21 differentially regulates DNA replication and DNA-repair-associated processes after UV irradiation. *J Cell Sci*. 2008 Oct 1;121(Pt 19):3271–3282. PubMed PMID: 18782865.
- [24] Mansilla SF, Bertolin AP, Bergoglio V, et al. Cyclin Kinase-independent role of p21(CDKN1A) in the promotion of nascent DNA elongation in unstressed cells. *Elife*. 2016 Oct 14;5. PubMed PMID: 27740454; PubMed Central PMCID: PMC5120883. DOI:10.7554/eLife.18020.
- [25] Maya-Mendoza A, Moudry P, Merchut-Maya JM, et al. High speed of fork progression induces DNA replication stress and genomic instability. *Nature*. 2018 Jul;559(7713):279–284. PubMed PMID: 29950726. DOI: 10.1038/s41586-018-0261-5.
- [26] Liu Y, Kwiatkowski DJ. Combined CDKN1A/TP53 mutation in bladder cancer is a therapeutic target. *Mol Cancer Ther*. 2015 Jan;14(1):174–182. PubMed PMID: 25349305; PubMed Central PMCID: PMC4297264. .
- [27] Origanti S, Cai SR, Munir AZ, et al. Synthetic lethality of Chk1 inhibition combined with p53 and/or p21 loss during a DNA damage response in normal and tumor cells. *Oncogene*. 2013 Jan 31;32(5):577–588. PubMed PMID: 22430210; PubMed Central PMCID: PMC3381958.
- [28] Petermann E, Woodcock M, Helleday T. Chk1 promotes replication fork progression by controlling replication initiation. *Proc Natl Acad Sci U S A*. 2010 Sep 14;107(37):16090–16095. PubMed PMID: 20805465; PubMed Central PMCID: PMC2941317. .
- [29] Syljuåsen RG, Sørensen CS, Hansen LT, et al. Inhibition of human Chk1 causes increased initiation of DNA replication, phosphorylation of ATR targets, and DNA breakage. *Mol Cell Biol*. 2005 May;25(9):3553–3562. PubMed PMID: 15831461; PubMed Central PMCID: PMC1084285.
- [30] Sørensen CS, Syljuåsen RG. Safeguarding genome integrity: the checkpoint kinases ATR, CHK1 and WEE1

- restrain CDK activity during normal DNA replication. *Nucleic Acids Res.* **2012** Jan;40(2):477–486. PubMed PMID: 21937510; PubMed Central PMCID: PMC3258124. .
- [31] Hasvold G, Lund-Andersen C, Lando M, et al. Hypoxia-induced alterations of G2 checkpoint regulators. *Mol Oncol.* **2016** May;10(5):764–773. PubMed PMID: 26791779; PubMed Central PMCID: PMC5423158.
- [32] Hauge S, Naucke C, Hasvold G, et al. Combined inhibition of Wee1 and Chk1 gives synergistic DNA damage in S-phase due to distinct regulation of CDK activity and CDC45 loading. *Oncotarget.* **2017** Feb 14;8(7):10966–10979. PubMed PMID: 28030798; PubMed Central PMCID: PMC5355238.
- [33] Tkacz-Stachowska K, Lund-Andersen C, Velissarou A, et al. The amount of DNA damage needed to activate the radiation-induced G2 checkpoint varies between single cells. *Radiother Oncol.* **2011** Oct;101(1):24–27. PubMed PMID: 21722983.
- [34] Ashley AK, Shrivastav M, Nie J, et al. DNA-PK phosphorylation of RPA32 Ser4/Ser8 regulates replication stress checkpoint activation, fork restart, homologous recombination and mitotic catastrophe. *DNA Repair (Amst).* **2014** Sep;21:131–139. PubMed PMID: 24819595; PubMed Central PMCID: PMC4135522.
- [35] Chen BP, Chan DW, Kobayashi J, et al. Cell cycle dependence of DNA-dependent protein kinase phosphorylation in response to DNA double strand breaks. *J Biol Chem.* **2005** Apr 15;280(15):14709–14715. PubMed PMID: 15677476.
- [36] Pfister SX, Markkanen E, Jiang Y, et al. Inhibiting Wee1 selectively kills histone h3k36me3-deficient cancers by dNTP starvation. *Cancer Cell.* **2015** Nov 9;28(5):557–568. PubMed PMID: 26602815; PubMed Central PMCID: PMC4643307.
- [37] Mak JP, Man WY, Ma HT, et al. Pharmacological targeting the ATR-CHK1-WEE1 axis involves balancing cell growth stimulation and apoptosis. *Oncotarget.* **2014** Nov 15;5(21):10546–10557. PubMed PMID: 25301733; PubMed Central PMCID: PMC4279392.
- [38] Rego MA, Harney JA, Mauro M, et al. Regulation of the activation of the Fanconi anemia pathway by the p21 cyclin-dependent kinase inhibitor. *Oncogene.* **2012** Jan 19;31(3):366–375. PubMed PMID: 21685936; PubMed Central PMCID: PMC3974337.
- [39] Yang Y, Gao Y, Mutter-Rottmayer L, et al. DNA repair factor RAD18 and DNA polymerase Polkappa confer tolerance of oncogenic DNA replication stress. *J Cell Biol.* **2017** Oct 2;216(10):3097–3115. PubMed PMID: 28835467; PubMed Central PMCID: PMC5626543.
- [40] Bridges KA, Hirai H, Buser CA, et al. MK-1775, a novel Wee1 kinase inhibitor, radiosensitizes p53-defective human tumor cells. *Clin Cancer Res.* **2011** Sep 1;17(17):5638–5648. PubMed PMID: 21799033; PubMed Central PMCID: PMC3167033.
- [41] Leijen S, Beijnen JH, Schellens JH. Abrogation of the G2 checkpoint by inhibition of Wee-1 kinase results in sensitization of p53-deficient tumor cells to DNA-damaging agents. *Curr Clin Pharmacol.* **2010** Aug;5(3):186–191. PubMed PMID: 20406171.
- [42] Leijen S, van Geel RM, Pavlick AC, et al. Phase I study evaluating WEE1 Inhibitor AZD1775 as monotherapy and in combination with gemcitabine, cisplatin, or carboplatin in patients with advanced solid tumors. *J Clin Oncol.* **2016** Dec 20;34(36):4371–4380. PubMed PMID: 27601554.
- [43] Leijen S, van Geel RM, Sonke GS, et al. Phase II study of WEE1 Inhibitor AZD1775 plus carboplatin in patients with TP53-mutated ovarian cancer refractory or resistant to first-line therapy within 3 months. *J Clin Oncol.* **2016** Dec 20;34(36):4354–4361. PubMed PMID: 27998224.
- [44] Rajeshkumar NV, De Oliveira E, Ottenhof N, et al. MK-1775, a potent Wee1 inhibitor, synergizes with gemcitabine to achieve tumor regressions, selectively in p53-deficient pancreatic cancer xenografts. *Clin Cancer Res.* **2011** May 1;17(9):2799–2806. PubMed PMID: 21389100; PubMed Central PMCID: PMC3307341.